

# Unsupervised Hashing via Similarity Distribution Calibration

Kam Woh Ng<sup>1,2</sup> Xiatian Zhu<sup>1,3</sup> Jiun Tian Hoe<sup>4</sup>  
 Chee Seng Chan<sup>5</sup> Tianyu Zhang Yi-Zhe Song<sup>1,2</sup> Tao Xiang<sup>1,2</sup>

<sup>1</sup>Centre for Vision, Speech and Signal Processing (CVSSP), University of Surrey

<sup>2</sup>iFlyTek-Surrey Joint Research Centre on Artificial Intelligence, University of Surrey

<sup>3</sup>Surrey Institute for People-Centred Artificial Intelligence, University of Surrey

<sup>4</sup>Nanyang Technological University

<sup>5</sup>Centre of Image and Signal Processing (CISiP), Universiti Malaya

{kamwoh.ng, xiatian.zhu, y.song, t.xiang}@surrey.ac.uk  
 jiuntian001@e.ntu.edu.sg  
 cs.chan@um.edu.my  
 macwish@hotmail.com

## Abstract

Existing unsupervised hashing methods typically adopt a feature similarity preservation paradigm. As a result, they overlook the intrinsic similarity capacity discrepancy between the continuous feature and discrete hash code spaces. Specifically, since the feature similarity distribution is intrinsically biased (e.g., moderately positive similarity scores on negative pairs), the hash code similarities of positive and negative pairs often become inseparable (i.e., the similarity collapse problem). To solve this problem, in this paper a novel **Similarity Distribution Calibration** (SDC) method is introduced. Instead of matching individual pairwise similarity scores, SDC aligns the hash code similarity distribution towards a calibration distribution (e.g., beta distribution) with sufficient spread across the entire similarity capacity/range, to alleviate the similarity collapse problem. Extensive experiments show that our SDC outperforms the state-of-the-art alternatives on both coarse category-level and instance-level image retrieval tasks, often by a large margin. Code is available at <https://github.com/kamwoh/sdc>.

## 1. Introduction

Hashing has been used extensively in real-world large-scale image retrieval systems. By converting continuous feature vectors into binary/discrete hash codes for indexing, hashing significantly reduces both computational cost

and memory footprint. Recent deep supervised learning to hash [6, 12, 31, 36, 38, 55, 63, 66] have greatly outperformed conventional methods [14, 20, 27, 29, 58]. However, supervised hashing is limited in scalability due to its reliance on a large quantity of labeled training data. A natural solution is to use *unsupervised hashing methods* instead, which do not require costly training data annotation.

The current state-of-the-art unsupervised hashing methods [32, 55] are based on *preserving individual pairwise similarities* between continuous feature vectors in the learned Hamming space. Compared to the alternative strategies (e.g., reconstruction [7], clustering [33], pseudo-labels [62], and contrastive learning [46]), pairwise similarity preservation is both easier to implement and more efficient, hence advantageous for large-scale applications [23].

However, for the first time, we point out that these similarity preservation-based hashing methods suffer from a **similarity collapse** problem as illustrated in Fig. 1b. That is, the hash code similarities of positive and negative pairs become inseparable. There are two causes: (i) The similarity distribution in the original continuous feature space is biased. In particular, most negative pairs take moderately positive similarity scores, as shown in Fig. 1a. (ii) The intrinsic similarity capacity discrepancy between the continuous feature and discrete hash code spaces. Here the capacity is defined as how fine-grained the similarity can be measured – The similarities between any two hash codes are of a fixed set of values determined by the code length (i.e., limited capacity), whilst the original feature similari-

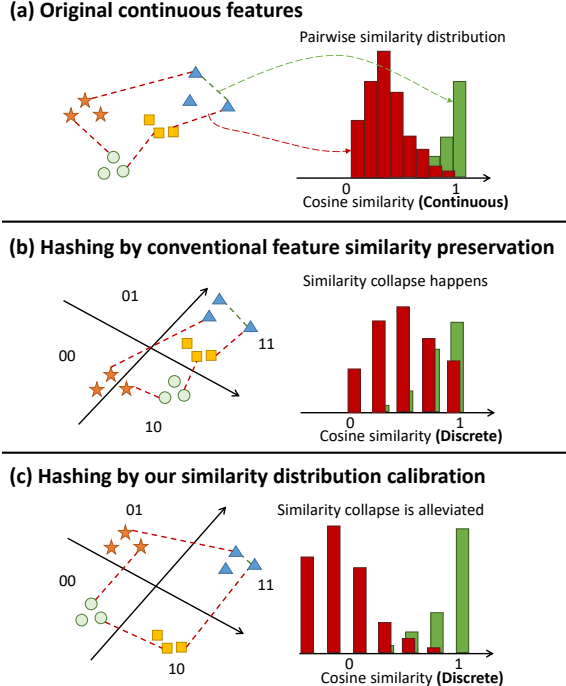


Figure 1. (a) Original continuous features (before hashing) and the cosine similarity distribution of positive (green) and negative (red) pairs. (b) After mapping to the hash code space under feature similarity preservation, the similarity collapse phenomenon happens due to the limited similarity capacity in Hamming space and the original similarity bias. (c) This problem can be well alleviated by our *Similarity Distribution Calibration* method.

ties are continuous (*i.e.*, unlimited capacity). With limited hash code similarity scores to map to, the hashing process is given little chance to recover from the collapsing positive and negative feature similarity scores in the Hamming space (Fig. 1b), resulting in inferior retrieval results.

To alleviate this similarity collapse problem, in this work a novel *Similarity Distribution Calibration* (**SDC**) method is introduced. Instead of preserving the original pairwise similarity scores individually, we match the hash code similarity distribution as a whole against a pre-defined calibration distribution (*e.g.*, beta distribution) with sufficient capacity range. Due to this stretching effect, the learned Hamming space is no longer restricted severely by the original biased similarity distribution as in the existing methods. This enables the limited similarity capacity of Hamming space to be better leveraged, resulting in improved performance (Fig. 1c).

We make the following **contributions**: (i) We reveal the fundamental similarity collapse problem suffered by existing pairwise similarity preservation-based unsupervised hashing methods. (ii) To address this problem, we propose

a Similarity Distribution Calibration (SDC) method by alleviating the severe restriction imposed by the original biased similarity scores. (iii) Extensive experiments validate the superiority of our SDC over state-of-the-art alternatives on four category-level and three instance-level image retrieval benchmarks.

## 2. Related Work

**Learning to hash.** Although earlier hashing methods [13, 14, 20, 24, 27, 40, 43, 58] are easy to apply in practice, their performance is typically inferior to more recent deep learning counterparts. Deep supervised hashing methods [6, 12, 31, 35, 36, 55, 57, 63, 66] usually achieve better performance over unsupervised ones by using additionally the semantic class labels. However, they are limited in scalability as class label annotation is costly and even impossible in extreme cases (*e.g.*, rare objects). Without this constraint, unsupervised methods are thus more scalable. Existing unsupervised hashing methods can be categorized into the following groups: similarity preservation [18, 19, 22, 29, 30, 32, 34, 39, 50, 55, 68], generative model [5, 10, 54, 70], reconstruction [7, 8, 51, 52], pseudo-labeling [15, 42, 60, 61, 67, 69], clustering [33, 65, 67, 69] and contrastive learning [33, 46, 64].

Among these, similarity preservation-based unsupervised hashing methods achieve the current state-of-the-art performance in image retrieval. They are also simple in design and efficient computationally. For example, PCA-H [24] and ITQ [14] project the features linearly into Hamming space which maximally preserves the original similarity. SSDH [60] and DistillHash [61] learn a hashing model with binary pairwise pseudo-labels inferred by the similarity scores. Instead, Binary Reconstructive Embeddings [29] optimizes a hash function by minimizing the difference between the Hamming distances and the original feature Euclidean distances on each training sample pair. Similarly, Angular Reconstructive Embeddings [18], Bi-half [32] and GreedyHash [55] all rely on minimizing the cosine similarity difference of training pairs across the hashing process. Despite the differences in their formulations, many of them suffer from the similarity collapse problem due to the common pairwise similarity preservation strategy adopted. *The objective of this work is to alleviate this limitation.*

**Separating positive and negative pairs in hashing.** MI-Hash [2, 3] maximizes the quality of a hash function with the mutual information between Hamming distances and pairwise labels during the learning. Similarly, RankMI [25] estimates the separation between distributions of positive similarities and negative similarities with mutual information and variational functions. However, both previous works rely on training labels which are absent in unsupervised hashing, making them inapplicable. Conceptually, we ex-

expand the advantages of separating positive and negative pairs from supervised hashing to the unsupervised setting by aligning with a prior distribution.

### 3. Methodology

To obtain a hash code  $b \in \{-1, +1\}^K$  with  $K$  bits, we need a hash function  $h$  as:

$$\mathbf{b} = h(\mathbf{x}) = \text{sign}(\phi(\mathbf{x})), \quad (1)$$

where  $\phi : \mathbf{x} \rightarrow \mathbf{f} \in \mathbb{R}^K$  is a (non-)linear mapping function compressing a  $d$ -dimensional feature vector  $\mathbf{x} \in \mathbb{R}^d$  into a  $K$ -dimensional continuous code  $\mathbf{f}$ .  $h$  is learned by optimizing an objective function  $\mathcal{L}$ . At test time for image retrieval, the Hamming distances between a query code,  $\mathbf{b}_p$ , and the gallery codes,  $\mathbf{b}_q$ , of a database can be mathematically computed as:

$$\mathcal{D}_h(\mathbf{b}_p, \mathbf{b}_q) = \frac{K}{2}(1 - \cos \theta_{pq}), \quad (2)$$

where  $\cos \theta_{pq} = \cos(\mathbf{b}_p, \mathbf{b}_q)$  is the cosine similarity between  $\mathbf{b}_p$  and  $\mathbf{b}_q$ .

The optimization is not differentiable when directly using Eq. (1) in a hashing objective  $\mathcal{L}$  due to the non-differentiable `sign` function. A straightforward solution is to remove the `sign` function, whilst minimizing the quantization error between  $\mathbf{f}$  and its hash code  $\mathbf{b}$  during training [41] as:

$$\mathcal{L}_q = \frac{1}{N} \sum_{i=1}^N (1 - \cos \theta_i), \quad \text{and} \quad \cos \theta_i = \cos(\mathbf{f}_i, \mathbf{b}_i), \quad (3)$$

where  $\cos \theta_i$  is the cosine similarity between the continuous code  $\mathbf{f}_i$  and the hash code counterpart  $\mathbf{b}_i = \text{sign}(\mathbf{f}_i)$  of  $i$ -th sample, and  $N$  specifies the training set size. This enables differentiable end-to-end hashing without a straight-through estimator [1, 55] or continuous relaxation [6]. Note, although the continuous codes  $\mathbf{f}$  are involved in learning, we describe the learning process directly with hash codes  $\mathbf{b}$  hereafter for convenience.

#### 3.1. Hashing by Conventional Similarity Preservation

Prior arts [14, 18, 20, 24, 29, 32, 55] preserve the pairwise similarities of the original continuous feature space during hashing. The loss function is often formulated as:

$$\mathcal{L}_p = \frac{1}{|\mathcal{N}|} \sum_{(i,j) \in \mathcal{N}} (t_{(i,j)} - s_{(i,j)})^2, \quad (4)$$

where  $t_{(i,j)} = \cos(\mathbf{x}_i, \mathbf{x}_j)$  is the similarity reconstruction target for a pair of samples  $\mathbf{x}_i$  and  $\mathbf{x}_j$  drawn from a training set  $\mathbf{X} \in \mathbb{R}^{N \times d}$ ,  $\mathcal{N}$  is a set of selected sample pairs,  $|\mathcal{N}|$  is

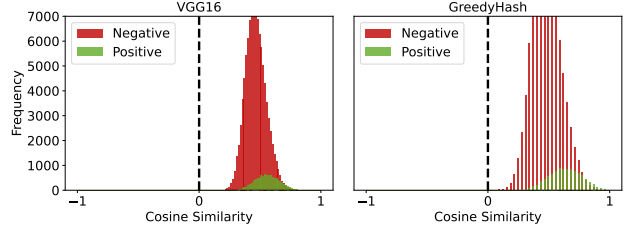


Figure 2. Pairwise similarity distribution of CIFAR10 using 100k randomly chosen negative pairs and 10k positive pairs. **(Left)** VGG16 features. **(Right)** 64-bits hash codes of GreedyHash [55]. Note that, the positive and negative labels are included for ease of explanation (*i.e.* descriptive purpose only), and were not deployed during the actual unsupervised training.

the cardinality of  $\mathcal{N}$ , and  $s_{(i,j)} = \cos(\mathbf{b}_i, \mathbf{b}_j)$  is the similarity of two hash codes. Each hash code is obtained with the hash function  $\mathbf{b} = h(\mathbf{x})$  (Eq. (1)).

As discussed earlier, similarity preservation-based unsupervised hashing methods suffer from a *similarity collapse* problem, as indicated by the severe overlapping in the hash code similarity scores of positive and negative pairs (Fig. 1b). Intuitively, this would lead to suboptimal retrieval performance.

As a concrete example, we examine the pairwise similarity distribution of CIFAR10 in the Hamming space. From Fig. 2 we observe that the distribution of hash code similarities is mainly concentrated in the positive region. This is because similarity preservation (*i.e.*, Eq. (4)) would directly inherit the similarity bias of the original feature space (VGG-16 features in this case). As a result, the similarity capacity of Hamming space is leveraged only at a limited degree, giving rise to the similarity collapse problem.

#### 3.2. Similarity Distribution Calibration

*Similarity Distribution Calibration* (SDC) is designed particularly for alleviating the similarity collapse problem. The idea is to align the empirical hash code similarity distribution of the training data with a calibration distribution with sufficient spread across the entire similarity capacity.

To measure the discrepancy between two probability distributions for similarity calibration, we adopt the Wasserstein distance with an elegant solution based on *inverse Cumulative Distribution Function* (iCDF) [47, 49]. Formally, we consider the hash code similarity  $s$  as a random variable with the iCDF  $F$ . Our Wasserstein distance-based calibration is formulated as:

$$\int_0^1 |F(z) - C(z)| dz, \quad (5)$$

where  $z$  is the quantile with the interval of  $[0, 1]$ , and  $C$  is the iCDF of the calibration distribution. The pipeline of SDC is depicted in Fig. 3.

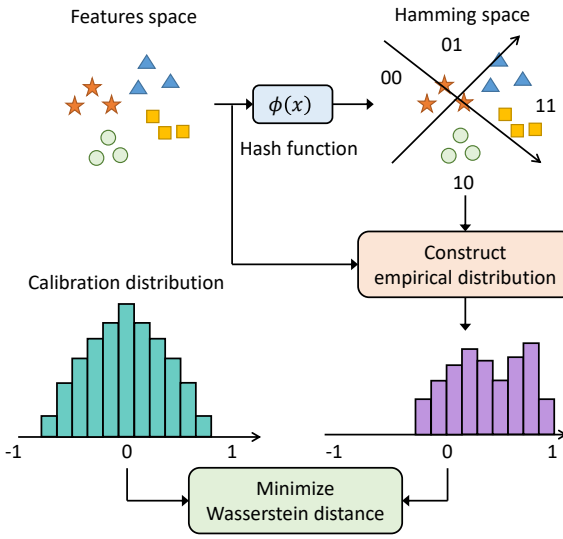


Figure 3. Pipeline of our proposed Similarity Distribution Calibration (SDC). We first map the original features into Hamming space through a learnable hash function. Next, we construct the empirical hash code similarity distribution. Finally, we minimize the Wasserstein distance between the empirical distribution and a calibration distribution.

### 3.2.1 Approximation

For mini-batch based deep learning, we can estimate  $F$  by collecting the pairwise similarities of hash codes and sorting them in the ascending order of *feature similarities*  $t$ . Due to the limited batch size, Eq. (5) needs to be approximated. Concretely, we evenly divide the probability range  $[0, 1]$  into  $|\mathcal{N}|$  bins and then aggregate per-bin calibration as:

$$\mathcal{L}_{\text{sdc}} = \frac{1}{|\mathcal{N}|} \sum_{s_i \in \mathcal{N}} |s_i - C\left(\frac{2i-1}{2|\mathcal{N}|}\right)|, \quad (6)$$

where  $s_i$  is  $i$ -th sorted hash code pairwise similarity. Orthogonal hash codes (*i.e.*,  $s = 0$ ) will produce maximum average Hamming distance [17]. We hence clip the negative part of  $C$ , which also helps improve training stability in practice.

### 3.2.2 Instantiation

In general, any distribution with sufficient capacity spread is a candidate for the calibration distribution. As an instantiation, we consider **beta distribution**,  $\text{Beta}(\alpha, \beta)$  with  $\alpha$  and  $\beta$  the two positive shape parameters. This is because its iCDF is bounded to the range  $[0, 1]$  so that it can be easily transformed to the target similarity range (*e.g.*,  $[-1, 1]$ )

---

### Algorithm 1: SDC Loss Function.

---

```

1  # phi: non-linear hash layer
2  # N: number of pairs (half of the batch)
3  # x: features (2N, d)
4
5  # compute continuous codes
6  f = phi(x) # (2N, k)
7
8  # construct pairs
9  xi, xj = x[:N], x[N:] # (N, d)
10 fi, fj = f[:N], f[N:] # (N, k)
11 t, t_idx = sort(cossim(xi, xj)) # (N, )
12 s = cossim(fi, fj) # (N, )
13
14 # sort with t's index
15 s = s[t_idx] # (N, )
16
17 # inverse CDF of beta distribution
18 C = beta.ppf(N, alpha=5, beta=5).relu() # (N, )
19
20 loss_sdc = (s - C).abs().mean()
21 loss_q = (1 - cossim(f, f.sign())).mean()
22 loss = loss_sdc + lambda_q * loss_q

```

---

for cosine similarity in our case). Other distributions (*e.g.*, Gaussian) can also be considered (see Table 4).

We set  $\alpha = \beta$  for simpler symmetric beta distribution. There is no prior knowledge about the optimal parameter value. However, as illustrated in Fig. 4b, the shapes of probability density functions (PDF) over different parameter values all seem to meet our requirements as calibration distribution. Empirically, we find that  $\alpha = \beta = 5$  work well overall (the default setting in experiments).

### 3.2.3 In the Hash Buckets Perspective

We justify the rationales of our SDC from the hash buckets perspective. It is assumed that an optimal hash function should encode similar items with the same hash code (preserved similarity) and fully utilize the Hamming space (decorrelated and balanced bit) [58]. In an ideal inverted file system [21],  $K$ -bits hash codes can form  $2^K$  hash buckets, and all the hash buckets should be utilized with equal size. Consequently, any two  $K$ -bits hash codes can be sampled with uniform probability.

Since the bits are balanced, the probability that one bit differs equals to 0.5. The probability that  $d$  bits differ<sup>1</sup> and  $K - d$  bits do not differ thus equals to  $(0.5)^d(0.5)^{K-d}$ . Next, the number of ways that only  $d$  bits differ equals to  $\binom{K}{d}$ . As a result, the probability that the Hamming distance between two uniformly sampled  $K$ -bits hash codes equals to  $d$  is:

$$\binom{K}{d} (0.5)^d (0.5)^{K-d} = \frac{1}{2^K} \binom{K}{d}. \quad (7)$$

This is equivalent to the probability mass function of a binomial distribution  $\text{B}(K, 0.5)$ . We plot the result in Fig. 4a

---

<sup>1</sup>This is also the Hamming distance.

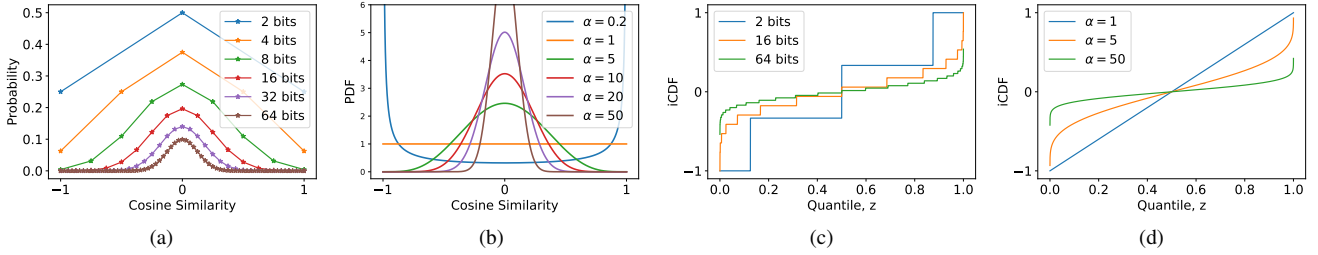


Figure 4. (updated) (a) Probability mass function (PMF) of  $B(K, 0.5)$  and (b) probability density function (PDF) of  $\text{Beta}(\alpha, \beta)$  distribution with different  $\alpha/\beta$  values. (c) Inverse cumulative density function (iCDF) of  $B(K, 0.5)$  and (d)  $\text{Beta}(\alpha, \beta)$  distribution with different  $\alpha/\beta$  values. Note that we set  $\alpha = \beta$  for symmetric PDF.

Methods	Venue	CIFAR10			ImageNet100			NUSWIDE			MS-COCO		
		16	32	64	16	32	64	16	32	64	16	32	64
LsH [20]	STOC'98	23.9	29.6	37.6	14.7	29.7	48.7	51.0	59.3	67.1	45.2	51.6	59.8
SH [58]	NeurIPS'08	41.8	42.1	43.5	35.1	50.9	60.9	63.0	60.9	64.0	59.4	64.8	66.2
PCA-H [24]	-	46.3	49.2	52.6	46.0	62.4	73.1	71.5	74.3	76.5	67.5	72.8	75.5
ITQ [14]	TPAMI'12	46.8	51.3	54.4	45.5	62.1	72.7	73.2	75.0	77.1	67.6	72.9	75.4
SSDH [60]	IJCAI'18	41.0	39.6	38.5	32.3	40.1	44.6	66.8	67.8	66.7	53.9	56.7	57.4
GreedyHash [55]	NeurIPS'18	44.9	51.9	55.7	54.4	68.7	74.7	70.0	76.2	79.3	66.8	73.2	77.4
TBH [52]	CVPR'20	48.2	50.2	50.7	42.9	44.5	48.3	75.8	77.8	78.5	68.8	72.6	74.8
CIBHash [46]	IJCAI'21	51.7	54.6	55.7	64.8	71.6	73.7	<b>79.4</b>	80.9	81.6	<b>75.5</b>	78.3	79.1
BiHalf [32]	AAAI'21	54.7	58.1	60.6	60.7	71.2	76.0	77.4	80.1	81.9	71.2	75.6	78.0
<b>SDC (Ours)</b>	-	<b>59.1</b>	<b>64.2</b>	<b>67.3</b>	<b>70.9</b>	<b>79.7</b>	<b>82.9</b>	79.1	<b>81.3</b>	<b>82.4</b>	75.3	<b>79.0</b>	<b>80.7</b>
<i>Original Features</i>	-	58.3			78.1			82.3			80.0		

Table 1. Coarse category-level image retrieval results of different unsupervised hashing methods with 3 different hash code lengths (16, 32, and 64). Note that PCA-H is ITQ before the quantization error minimization. The last row reports the results of the original 4096d VGG-16 [53] features with the cosine similarity.

and the iCDF of Eq. (7) in Fig. 4c. From both figures, we see that as  $K$  varies from 2-bits to 64-bits, the similarity distribution is similar to the beta distribution with  $\alpha = \beta \rightarrow \infty$  (see Fig. 4d). This means that for learning an optimal hash function, we should produce hash codes with their pairwise similarity distribution similar to a binomial distribution. In case that the Hamming space is not fully used, there should exist imbalanced hash bucket sizes, corresponding to a biased similarity distribution — similarity collapse emerges.

### 3.2.4 Remarks

Note that the feature similarity scores are used to sort the hash code counterparts while constructing the iCDF. However, unlike the conventional strategy preserving *individual* pairwise similarity scores rigidly, our SDC leverages the distribution of feature similarity scores *holistically*.

In practice, we observe that the pairwise feature similarities could vary over mini-batches. During calibration, we apply sorting to rank them before aligning their corresponding hash code similarities with the prior distribution. As a result, our method does not seek a one-to-one alignment between feature similarity and prior distribution. This

property could be understood as a type of stochastic noise during optimization, in the spirit of SGD optimization.

### 3.3. Overall Learning Objective

For model training, we deploy the overall objective loss function as:

$$\mathcal{L} = \mathcal{L}_{\text{sdc}} + \lambda_q \mathcal{L}_q, \quad (8)$$

where  $\mathcal{L}_q$  is the quantization loss as defined in Eq. (3), and  $\lambda_q$  is a weight hyper-parameter. We simply set  $\lambda_q = 1$  unless mentioned otherwise. The algorithm is depicted in Alg. 1.

## 4. Experiments

**Datasets.** We consider both coarse category-level and fine-grained instance-level image retrieval tasks in our experiments. Following [12, 32, 46, 52, 55], we use 4 category-level datasets: i) **CIFAR-10** [28], ii) **NUS-WIDE** [9], and iii) **MS-COCO** [37]. With an ImageNet pre-trained model, we also choose iv) **ImageNet100** (a subset of ImageNet [11] as first used by [6] and later by supervised deep hashing

Methods	ResNet50 [16]				DeiT-S [56]			
	CIFAR10	ImageNet100	NUSWIDE	MS-COCO	CIFAR10	ImageNet100	NUSWIDE	MS-COCO
ITQ [14]	64.6	73.9	79.5	75.3	80.4	74.7	79.2	78.4
GreedyHash [55]	61.4	77.9	83.0	77.6	81.5	79.7	80.8	80.8
BiHalf [32]	76.6	80.4	82.7	78.5	79.9	<b>81.3</b>	74.5	79.7
<b>SDC (Ours)</b>	<b>78.7</b>	<b>85.1</b>	<b>83.7</b>	<b>81.3</b>	<b>89.5</b>	80.7	<b>83.3</b>	<b>82.9</b>
<i>Original Features</i>	69.3	81.8	83.9	82.1	82.3	82.5	83.9	84.2

Table 2. Coarse category-level image retrieval results of representative unsupervised hashing methods on ImageNet100. 64-bits hash codes are used. The last row reports the results of the original 2048d ResNet50 and 384d DeiT-S features.

works), which was ignored by previous unsupervised hashing works. For evaluating instance-level retrieval tasks, three popular datasets are chosen including i) **GLDv2** [59], ii) **ROxif** [44, 48], and iii) **RParis** [45, 48].

**Evaluation metrics.** Following previous works [32, 46, 55], we measure the model performance with mean Average Precision (mAP) at top 1000 (mAP@1K) for single-labeled datasets (*i.e.*, ImageNet100 and CIFAR10), while top 5000 (mAP@5K) for multi-labeled datasets (*i.e.*, NUS-WIDE and MS-COCO). Note, for instance-level retrieval tasks, we follow the evaluation protocol of [4, 17] and use mAP@100 as the evaluation metric. For statistical stability, we run 3 trials for each experiment and report the average of per-trial best results on the validation set. In addition, we also plot Precision-Recall curves (PR) to compare the precisions at different recall rates.

**Competitors.** We compare our method with 4 classic unsupervised hashing methods [14, 20, 24, 58] still considered as strong baselines, and 5 recent SOTA unsupervised deep hashing methods [32, 46, 52, 55, 60].

**Implementation details.** For fair comparisons, we follow the existing experimental protocol [32, 46, 52, 55]. We use an ImageNet pre-trained VGG-16 [53] as the fixed and frozen feature extractor for main experiments, as the focus of our evaluation is on the hashing model. For more extensive evaluation, we also additionally use pre-trained ResNet50 [16] and DeiT [56]. We test three common code lengths: 16, 32, and 64 bits. We train all the compared methods using Adam [26] optimizer for 100 epochs with a learning rate of 0.0001 and a batch size of 64, with a single exception in TBH [52], for which a batch size of 400 is used and 1000 epochs are required. Note that we reimplemented all competing methods based on the original released codes. Our reimplementation can reproduce the reported performances under the original setting. This allows us to evaluate all the models fairly under a single setting sharing the same datasets, testing protocols, and network architectures. More experimental details including the training/query/gallery splits for each dataset and implementation details are given in the supplementary material.

## 4.1. Comparative Results

**Coarse category-level retrieval results.** We report the

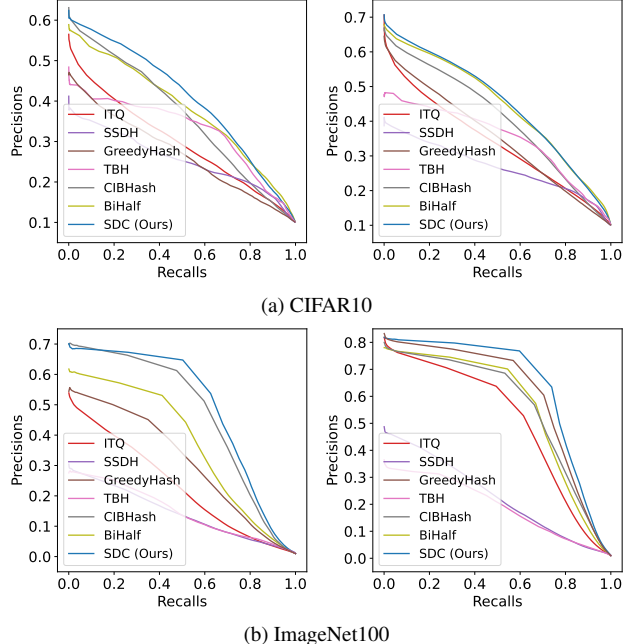


Figure 5. PR curve on CIFAR10 and ImageNet100. Left and right figures correspond to 16-bits and 64-bits hash codes.

retrieval results of our SDC and prior art unsupervised hashing methods on three different datasets in Table 1. It is evident that our SDC outperforms significantly the best competitors (*e.g.*, BiHalf and CIBHash), especially in the low bit (*e.g.*, 16) cases, *e.g.*, by up to 6.7%, and 10.2% on CIFAR10 and ImageNet100 respectively. In terms of training efficiency, with heavy data augmentation on raw training data, CIBHash needs to take *hours* for training on a single GTX 3070 GPU (*e.g.*, about 60 seconds per epoch and totally about 1.6 hours for ImageNet100). In contrast, both BiHalf and our SDC can use pre-extracted features with the training taking *only minutes* (*e.g.*, about 4 seconds per epoch and 7 minutes in total for ImageNet100).

We also report PR curves in Fig. 5. It can be observed that our SDC (blue curves) consistently outperforms all competing methods, especially at low bit cases (*i.e.*, 16-bits). This suggests that our SDC can learn hash codes for superior image retrieval across different recall rates.

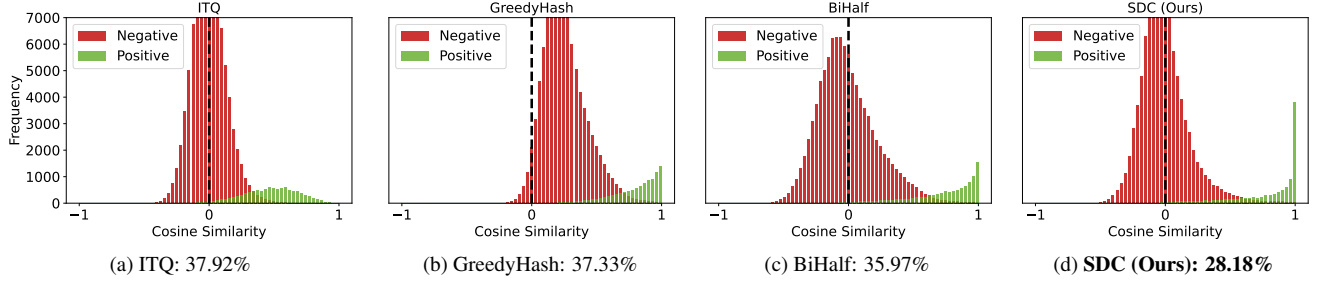


Figure 6. Analysis of the similarity collapse problem on ImageNet100. We plot the hamming distance histograms for 10000 positive and 100000 negative random pairs with 64-bits hash codes. For similarity collapse quantification, we use the intersection between the two histograms as the metric, lower is better. Note that, the positive and negative labels are included for ease of explanation (*i.e.* descriptive purpose only), and were not deployed during the actual unsupervised training.

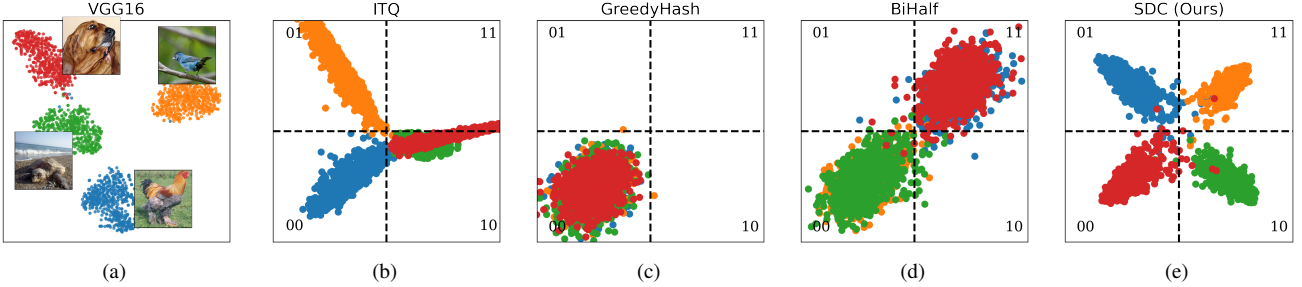


Figure 7. (a) The t-SNE visualization of VGG16 features of 4 selected classes of ImageNet100. (b-e) Continuous 2-bit codes before quantization derived by different unsupervised hashing methods. Dotted lines denote the separation of Hamming space.

Methods	GLDv2		$\mathcal{R}\text{Oxf}$		$\mathcal{R}\text{Paris}$	
	128	512	128	512	128	512
ITQ [14]	5.2	11.3	1.6	5.4	4.8	12.3
GreedyHash [55]	3.8	7.9	15.8	34.2	34.9	52.8
BiHalf [32]	4.0	6.7	20.2	33.3	42.0	52.0
<b>SDC (Ours)</b>	<b>6.3</b>	<b>12.1</b>	<b>27.1</b>	<b>40.8</b>	<b>50.3</b>	<b>63.8</b>
Original features	13.8		51.0		71.5	

Table 3. Instance-level image retrieval results of representative unsupervised hashing methods on GLDv2,  $\mathcal{R}\text{Oxf-Hard}$  and  $\mathcal{R}\text{Paris-Hard}$ . Original features: 2048D R50-DELG features [4] with the cosine similarity.

**Different feature representations.** For more extensive evaluation, we further evaluate two stronger feature models: ResNet50 [16] and DeiT-Small [56]. Table 2 shows that our SDC again outperforms the strong competitors ITQ and Bihalf. This suggests that the advantage of our method is feature representation agnostic.

**Instance-level retrieval results.** We also evaluate our model on instance-level image retrieval tasks. We follow the evaluation protocol of [17]<sup>2</sup>. We use three datasets, namely GLDv2 [59],  $\mathcal{R}\text{Oxf}$ , and  $\mathcal{R}\text{Paris}$  [48]. Note, due to no training data with  $\mathcal{R}\text{Oxf}$  and  $\mathcal{R}\text{Paris}$ , we use the train-

ing set of GLDv2 for model training for all datasets. As shown in Table 3, our SDC still outperforms consistently the state-of-the-art similarity preservation based methods (*i.e.*, GreedyHash [55], and BiHalf [32]) by a large margin. This indicates that the superiority of our SDC generalizes from coarse category retrieval to fine-grained instance retrieval, even in the presence of a distributional shift between the training and test sets.

## 4.2. Further Analysis

**Similarity collapse analysis.** We first examine the similarity collapse problem. We study three representative hashing methods (ITQ, GreedyHash, Bihalf) in comparison with our SDC. To quantify this collapse, we compute the intersection between the cosine similarity histogram of positive and negative pairs. Higher intersection rates suggest worse collapses with lower discriminating ability. We use 64-bits hash codes. To compute the two histograms, we sample 10k positive and 100k negative random pairs of ImageNet100. Fig. 6 presents the degree of similarity collapse in the order of ITQ > GreedyHash > BiHalf > SDC. This verifies again that our method is most effective in alleviating this collapse problem.

**Hash code visualization.** For further examination, we visualize continuous hash codes in a proof-of-concept setting.

<sup>2</sup>Please see supplementary material for implementation details.

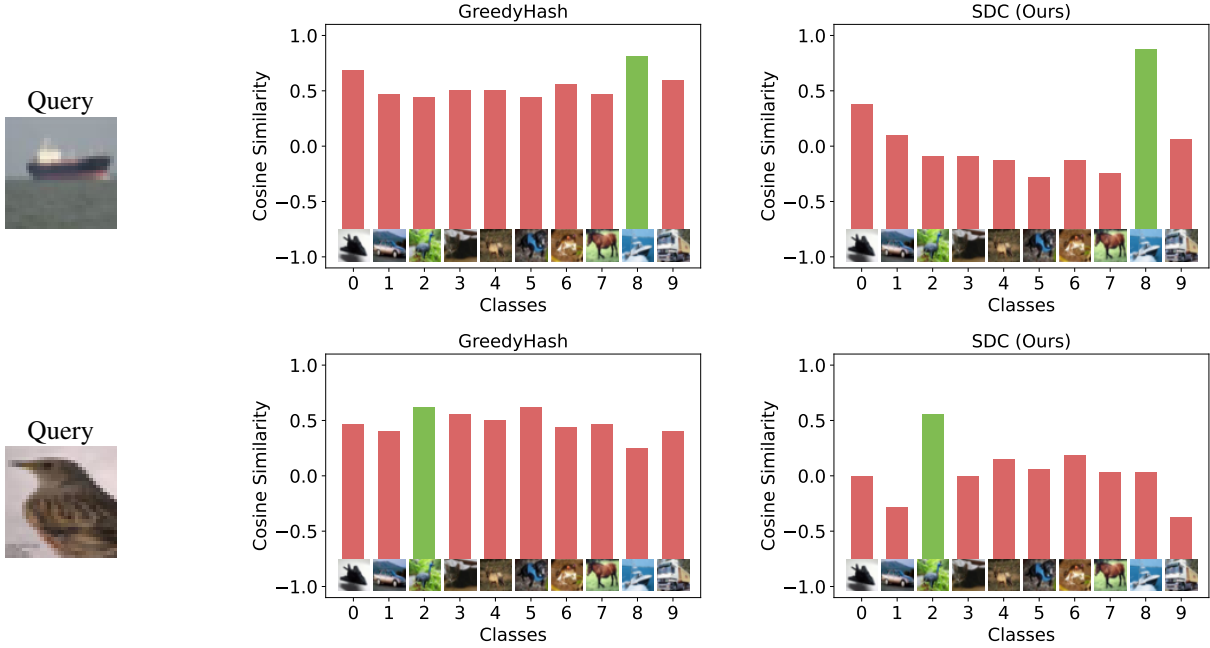


Figure 8. Two qualitative object image retrieval examples on CIFAR10. Green: Positive class; Red: Negative class.

Specifically, we examine the behaviour of ITQ, Greedy-Hash, BiHalf and SDC in learning a 2-bits hash function over 4 object classes (cock, indigo-bunting, loggerhead, bloodhound) from ImageNet100. We use the VGG-16 features. We observe from Fig. 7 that whilst the original features are already well separable, different methods behave differently. For example, simply preserving the original similarity, GreedyHash collapses the similarity scores completely across all the classes. With a code balance layer on top, BiHalf partly reduces the degree of collapsing to two groups. Through aligning the similarity distribution with a calibration distribution, our SDC solves this collapsing problem well, even further separating the originally confusing two classes (cock and bloodhound). This validates the unexceptional potential of SDC in improving over the original continuous features.

**Qualitative evaluation.** For visual analysis, we provide a couple of image retrieval examples on CIFAR10. It is evident in Fig. 8 that our SDC can identify the positive class more confidently with a more distinctive separation between positive and negative classes compared to Greedy-Hash. This indicates the superior discrimination ability of our similarity distribution calibration idea in unsupervised hashing.

### 4.3. Ablation Study

**Calibration distribution.** We evaluate the effect of calibration distribution. We further test normalized Gaussian distribution (bounded within  $[-1, 1]$ ) as well as a variety of

Distributions	CIFAR10	ImageNet100	GLDv2
Beta(0.2, 0.2)	62.2	79.7	11.6
Beta(0.5, 0.5)	63.6	80.6	11.9
Beta(0.7, 0.7)	64.1	80.8	11.8
Beta(1, 1)	66.2	80.8	12.0
Beta(2, 2)	67.0	81.4	<b>12.1</b>
Beta(3, 3)	<b>67.3</b>	81.9	12.0
Beta(5, 5)	<b>67.3</b>	82.9	<b>12.1</b>
Beta(7, 7)	66.8	82.8	11.8
Beta(10, 10)	65.9	<b>83.3</b>	11.8
Gaussian	<b>67.3</b>	82.3	11.5

Table 4. Effect of the calibration distribution. *Setting:* 64-bits hash codes on CIFAR10 and ImageNet and 512-bits on GLDv2.

Beta distributions. We observe in Table 4 that (1) The performance Beta calibration is generally stable in the range of  $[2, 5]$ ; (2) Gaussian calibration is similarly effective suggesting the flexibility of our SDC in distribution selection.

**Orthogonality.** We evaluate the effect of orthogonality with our SDC loss design (Section 3.2.1). It is shown in Table 5 that the orthogonality constraint is useful, confirming our design choice and also echoing a similar finding as [17].

## 5. Conclusion

We have presented a simple yet effective *Similarity Distribution Calibration* (SDC) method for unsupervised hashing. This is particularly designed to alleviate the largely ig-

Orthogonality Constraint	CIFAR10	ImageNet100	GLDv2
No	64.9	81.1	7.2
Yes	<b>67.3</b>	<b>82.9</b>	<b>12.1</b>

Table 5. Effect of orthogonality. *Setting*: 64-bits hash codes on CIFAR10 and ImageNet and 512-bits on GLDv2.

nored *similarity collapse* problem suffered by the existing similarity preservation-based unsupervised hashing methods. Concretely, we minimize the Wasserstein distance between the distribution of Hamming similarities and a calibration distribution with a sufficient capacity range. As a result, the low similarity capacity of hash code can be better exploited for improved discriminating ability. Extensive experiments on both coarse and fine-grained image retrieval tasks validated the advantage of our method over the state-of-the-art alternatives.

## References

[1] Yoshua Bengio, Nicholas Léonard, and Aaron Courville. Estimating or propagating gradients through stochastic neurons for conditional computation. *arXiv preprint arXiv:1308.3432*, 2013. 3

[2] Fatih Cakir, Kun He, Sarah A. Bargal, and Stan Sclaroff. Mihash: Online hashing with mutual information. In *International Conference on Computer Vision*, 2017. 2

[3] Fatih Cakir, Kun He, Sarah Adel Bargal, and Stan Sclaroff. Hashing with mutual information. *IEEE Transactions on Pattern Analysis and Machine Intelligence*, 2019. 2

[4] Bingyi Cao, André Araujo, and Jack Sim. Unifying deep local and global features for image search. In *European Conference on Computer Vision*, 2020. 6, 7

[5] Yue Cao, Bin Liu, Mingsheng Long, and Jianmin Wang. Hashgan: Deep learning to hash with pair conditional wasserstein gan. In *Computer Vision and Pattern Recognition*, 2018. 2

[6] Zhangjie Cao, Mingsheng Long, Jianmin Wang, and Philip S. Yu. Hashnet: Deep learning to hash by continuation. In *International Conference on Computer Vision*, 2017. 1, 2, 3, 5

[7] Miguel A Carreira-Perpinán and Ramin Raziperchikolaei. Hashing with binary autoencoders. In *Computer Vision and Pattern Recognition*, 2015. 1, 2

[8] Junjie Chen, William K Cheung, and Anran Wang. Learning deep unsupervised binary codes for image retrieval. In *International Joint Conference on Artificial Intelligence*, 2018. 2

[9] Tat-Seng Chua, Jinhui Tang, Richang Hong, Haojie Li, Zhiping Luo, and Yan-Tao Zheng. Nus-wide: A real-world web image database from national university of singapore. In *Conference on Image and Video Retrieval*, 2009. 5

[10] Bo Dai, Ruiqi Guo, Sanjiv Kumar, Niao He, and Le Song. Stochastic generative hashing. In *International Conference on Machine Learning*, 2017. 2

[11] Jia Deng, Wei Dong, Richard Socher, Li-Jia Li, Kai Li, and Li Fei-Fei. Imagenet: A large-scale hierarchical im-

age database. In *Computer Vision and Pattern Recognition*, 2009. 5

[12] Lixin Fan, Kam Woh Ng, Ce Ju, Tianyu Zhang, and Chee Seng Chan. Deep polarized network for supervised learning of accurate binary hashing codes. In *International Joint Conference on Artificial Intelligence*, 2020. 1, 2, 5

[13] Yunchao Gong, Sanjiv Kumar, Vishal Verma, and Svetlana Lazebnik. Angular quantization-based binary codes for fast similarity search. In *Advances in Neural Information Processing Systems*, 2012. 2

[14] Yunchao Gong, Svetlana Lazebnik, Albert Gordo, and Florent Perronnin. Iterative quantization: A procrustean approach to learning binary codes for large-scale image retrieval. *IEEE Transactions on Pattern Analysis and Machine Intelligence*, 2012. 1, 2, 3, 5, 6, 7

[15] Yifan Gu, Haofeng Zhang, Zheng Zhang, and Qiaolin Ye. Unsupervised deep triplet hashing with pseudo triplets for scalable image retrieval. *Multimedia Tools and Applications*, 2019. 2

[16] Kaiming He, Xiangyu Zhang, Shaoqing Ren, and Jian Sun. Deep residual learning for image recognition. In *Computer Vision and Pattern Recognition*, 2016. 6, 7

[17] Juiun Tian Hoe, Kam Woh Ng, Tianyu Zhang, Chee Seng Chan, Yi-Zhe Song, and Tao Xiang. One loss for all: Deep hashing with a single cosine similarity based learning objective. In *Advances in Neural Information Processing Systems*, 2021. 4, 6, 7, 8

[18] Mengqiu Hu, Yang Yang, Fumin Shen, Ning Xie, and Heng Tao Shen. Hashing with angular reconstructive embeddings. *IEEE Transactions on Image Processing*, 2018. 2, 3

[19] Shanshan Huang, Yichao Xiong, Ya Zhang, and Jia Wang. Unsupervised triplet hashing for fast image retrieval. In *Thematic Workshops of ACM Multimedia*, 2017. 2

[20] Piotr Indyk and Rajeev Motwani. Approximate nearest neighbors: Towards removing the curse of dimensionality. In *Annual ACM Symposium on Theory of Computing*, 1998. 1, 2, 3, 5, 6

[21] Herve Jegou, Matthijs Douze, and Cordelia Schmid. Product quantization for nearest neighbor search. *IEEE Transactions on Pattern Analysis and Machine Intelligence*, 2010. 4

[22] Sheng Jin, Hongxun Yao, Xiaoshuai Sun, and Shangchen Zhou. Unsupervised semantic deep hashing. *Neurocomputing*, 2019. 2

[23] Jeff Johnson, Matthijs Douze, and Hervé Jégou. Billion-scale similarity search with gpus. *IEEE Transactions on Big Data*, 2021. 1

[24] Ian Jolliffe. Principal component analysis and factor analysis. *Principal Component Analysis*, 1986. 2, 3, 5, 6

[25] Mete Kemertas, Leila Pishdad, Konstantinos G Derpanis, and Afsaneh Fazly. Rankmi: A mutual information maximizing ranking loss. In *Computer Vision and Pattern Recognition*, 2020. 2

[26] Diederik P Kingma and Jimmy Ba. Adam: A method for stochastic optimization. In *International Conference on Learning Representations*, 2015. 6

[27] Weihao Kong and Wu-jun Li. Isotropic hashing. In *Advances in Neural Information Processing Systems*, 2012. 1, 2

[28] Alex Krizhevsky and Geoffrey Hinton. Learning multiple layers of features from tiny images. Technical report, University of Toronto, 2009. 5

[29] Brian Kulis and Trevor Darrell. Learning to hash with binary reconstructive embeddings. In *Advances in Neural Information Processing Systems*, 2009. 1, 2, 3

[30] Shuyan Li, Zhixiang Chen, Jiwen Lu, Xiu Li, and Jie Zhou. Neighborhood preserving hashing for scalable video retrieval. In *International Conference on Computer Vision*, 2019. 2

[31] Wu-Jun Li, Sheng Wang, and Wang-Cheng Kang. Feature learning based deep supervised hashing with pairwise labels. In *International Joint Conference on Artificial Intelligence*, 2016. 1, 2

[32] Yunqiang Li and Jan van Gemert. Deep unsupervised image hashing by maximizing bit entropy. In *AAAI Conference on Artificial Intelligence*, 2021. 1, 2, 3, 5, 6, 7

[33] Yang Li, Yapeng Wang, Zhuang Miao, Jiabao Wang, and Rui Zhang. Contrastive self-supervised hashing with dual pseudo agreement. *IEEE Access*, 2020. 1, 2

[34] Kevin Lin, Jiwen Lu, Chu-Song Chen, and Jie Zhou. Learning compact binary descriptors with unsupervised deep neural networks. In *Computer Vision and Pattern Recognition*, 2016. 2

[35] Mingbao Lin, Rongrong Ji, Hong Liu, Xiaoshuai Sun, Shen Chen, and Qi Tian. Hadamard matrix guided online hashing. *International Journal of Computer Vision*, 2020. 2

[36] Mingbao Lin, Rongrong Ji, Hong Liu, and Yongjian Wu. Supervised online hashing via hadamard codebook learning. In *ACM International Conference on Multimedia*, 2018. 1, 2

[37] Tsung-Yi Lin, Michael Maire, Serge Belongie, James Hays, Pietro Perona, Deva Ramanan, Piotr Dollár, and C. Lawrence Zitnick. Microsoft coco: Common objects in context. In *European Conference on Computer Vision*, 2014. 5

[38] Bin Liu, Yue Cao, Mingsheng Long, Jianmin Wang, and Jingdong Wang. Deep triplet quantization. In *ACM International Conference on Multimedia*, 2018. 1

[39] Wei Liu, Cun Mu, Sanjiv Kumar, and Shih-Fu Chang. Discrete graph hashing. In *Advances in Neural Information Processing Systems*, 2014. 2

[40] Wei Liu, Jun Wang, Rongrong Ji, Yu-Gang Jiang, and Shih-Fu Chang. Supervised hashing with kernels. In *Computer Vision and Pattern Recognition*, 2012. 2

[41] Xiao Luo, Daqing Wu, Chong Chen, Minghua Deng, Jian-qiang Huang, and Xian-Sheng Hua. A survey on deep hashing methods. *arXiv preprint arXiv:2003.03369*, 2020. 3

[42] Xiao Luo, Daqing Wu, Zeyu Ma, Chong Chen, Minghua Deng, Jinwen Ma, Zhongming Jin, Jianqiang Huang, and Xian-Sheng Hua. Cimon: Towards high-quality hash codes. In *International Joint Conference on Artificial Intelligence*, 2021. 2

[43] Mohammad Norouzi, David J Fleet, and Russ R Salakhutdinov. Hamming distance metric learning. In *Advances in Neural Information Processing Systems*, 2012. 2

[44] James Philbin, Ondrej Chum, Michael Isard, Josef Sivic, and Andrew Zisserman. Object retrieval with large vocabularies and fast spatial matching. In *Computer Vision and Pattern Recognition*, 2007. 6

[45] James Philbin, Ondrej Chum, Michael Isard, Josef Sivic, and Andrew Zisserman. Lost in quantization: Improving particular object retrieval in large scale image databases. In *Computer Vision and Pattern Recognition*, 2008. 6

[46] Zexuan Qiu, Qinliang Su, Zijing Ou, Jianxing Yu, and Changyou Chen. Unsupervised hashing with contrastive information bottleneck. In *International Joint Conference on Artificial Intelligence*, 2021. 1, 2, 5, 6

[47] Julien Rabin, Gabriel Peyré, Julie Delon, and Marc Bernot. Wasserstein barycenter and its application to texture mixing. In *International Conference on Scale Space and Variational Methods in Computer Vision*. Springer, 2011. 3

[48] Filip Radenovic, Ahmet Iscen, Giorgos Tolias, Yannis Avrithis, and Ondrej Chum. Revisiting oxford and paris: Large-scale image retrieval benchmarking. In *Computer Vision and Pattern Recognition*, 2018. 6, 7

[49] Aaditya Ramdas, Nicolás García Trillo, and Marco Cuturi. On wasserstein two-sample testing and related families of nonparametric tests. *Entropy*, 2017. 3

[50] Fumin Shen, Yan Xu, Li Liu, Yang Yang, Zi Huang, and Heng Tao Shen. Unsupervised deep hashing with similarity-adaptive and discrete optimization. *IEEE Transactions on Pattern Analysis and Machine Intelligence*, 2018. 2

[51] Yuming Shen, Li Liu, and Ling Shao. Unsupervised binary representation learning with deep variational networks. *International Journal of Computer Vision*, 2019. 2

[52] Yuming Shen, Jie Qin, Jiaxin Chen, Mengyang Yu, Li Liu, Fan Zhu, Fumin Shen, and Ling Shao. Auto-encoding twin-bottleneck hashing. In *Computer Vision and Pattern Recognition*, 2020. 2, 5, 6

[53] Karen Simonyan and Andrew Zisserman. Very deep convolutional networks for large-scale image recognition, 2015. 5, 6

[54] Jingkuan Song, Tao He, Lianli Gao, Xing Xu, Alan Hanjalic, and Heng Tao Shen. Binary generative adversarial networks for image retrieval. In *AAAI Conference on Artificial Intelligence*, 2018. 2

[55] Shupeng Su, Chao Zhang, Kai Han, and Yonghong Tian. Greedy hash: Towards fast optimization for accurate hash coding in cnn. In *Advances in Neural Information Processing Systems*, 2018. 1, 2, 3, 5, 6, 7

[56] Hugo Touvron, Matthieu Cord, Matthijs Douze, Francisco Massa, Alexandre Sablayrolles, and Hervé Jégou. Training data-efficient image transformers & distillation through attention. In *International Conference on Machine Learning*. PMLR, 2021. 6, 7

[57] Xiaofang Wang, Yi Shi, and Kris M Kitani. Deep supervised hashing with triplet labels. In *Asian Conference on Computer Vision*, 2016. 2

[58] Yair Weiss, Antonio Torralba, and Rob Fergus. Spectral hashing. In *Advances in Neural Information Processing Systems*, 2009. 1, 2, 4, 5, 6

[59] Tobias Weyand, Andre Araujo, Bingyi Cao, and Jack Sim. Google landmarks dataset v2-a large-scale benchmark for instance-level recognition and retrieval. In *Computer Vision and Pattern Recognition*, 2020. 6, 7

[60] Erkun Yang, Cheng Deng, Tongliang Liu, Wei Liu, and Dacheng Tao. Semantic structure-based unsupervised deep hashing. In *International Joint Conference on Artificial Intelligence*, 2018. 2, 5, 6

[61] Erkun Yang, Tongliang Liu, Cheng Deng, Wei Liu, and Dacheng Tao. Distillhash: Unsupervised deep hashing by distilling data pairs. In *Computer Vision and Pattern Recognition*, 2019. 2

[62] Huei-Fang Yang, Kevin Lin, and Chu-Song Chen. Supervised learning of semantics-preserving hash via deep convolutional neural networks. *IEEE Transactions on Pattern Analysis and Machine Intelligence*, 2017. 1

[63] Zhan Yang, Osolo Ian Raymond, Wuqing Sun, and Jun Long. Deep attention-guided hashing. *IEEE Access*, 2019. 1, 2

[64] Jiaguo Yu, Yuming Shen, Haofeng Zhang, Philip H. S. Torr, and Menghan Wang. Learning to hash naturally sorts. In *International Joint Conference on Artificial Intelligence*, 2022. 2

[65] Shuying Yu, Xian-Ling Mao, Wei Wei, and Heyan Huang. Unsupervised deep hashing via adaptive clustering. In *Asia-Pacific Web (APWeb) and Web-Age Information Management (WAIM) Joint International Conference on Web and Big Data*, 2021. 2

[66] Li Yuan, Tao Wang, Xiaopeng Zhang, Francis EH Tay, Ze-qun Jie, Wei Liu, and Jiashi Feng. Central similarity quantization for efficient image and video retrieval. In *Computer Vision and Pattern Recognition*, 2020. 1, 2

[67] Wanqian Zhang, Dayan Wu, Yu Zhou, Bo Li, Weiping Wang, and Dan Meng. Deep unsupervised hybrid-similarity hadamard hashing. In *ACM International Conference on Multimedia*, 2020. 2

[68] Kang Zhao, Hongtao Lu, and Jincheng Mei. Locality preserving hashing. In *AAAI Conference on Artificial Intelligence*, 2014. 2

[69] Yuxuan Zhu, Yali Li, and Shengjin Wang. Unsupervised deep hashing with adaptive feature learning for image retrieval. *IEEE Signal Processing Letters*, 2019. 2

[70] Maciej Zieba, Piotr Semberecki, Tarek El-Gaaly, and Tomasz Trzcinski. Bingan: Learning compact binary descriptors with a regularized gan. In *Proceedings of Advances in Neural Information Processing Systems*, 2018. 2